Biochemical Characterization of the Minichromosome Maintenance (MCM) Protein of the Crenarchaeote *Aeropyrum pernix* and Its Interactions with the Origin Recognition Complex (ORC) Proteins[†]

Neli Atanassova[‡] and Ian Grainge*

Cancer Research UK Clare Hall Laboratories, The London Research Institute, Blanche Lane, South Mimms, Potters Bar, Herts EN6 3LD, U.K.

Received August 6, 2008; Revised Manuscript Received October 2, 2008

ABSTRACT: Replication in archaea is carried out by proteins that are homologues of eukaryotic counterparts. However, the archaeal systems tend to be much simpler with fewer different genes encoding the core functions than in eukaryotic counterparts. In many archaea, there is a single minichromosome maintenance (MCM) homologue, presumed to be the replicative helicase and between one and three origin recognition complex (ORC) homologues involved in binding to the replication origins. Here we describe the cloning and characterization of the MCM protein from the crenarchaeote *Aeropyrum pernix*. Like other eukaryotic and archaeal MCM proteins, it is found to be an ATP-dependent DNA helicase, and the putative active site residues involved in ATP binding and hydrolysis are confirmed by mutation. Deletion of the N-terminal 256 amino acids yielded a protein with higher ATPase activity in the absence of DNA and retained robust helicase activity. Interactions with the ORC proteins of *A. pernix* were examined, and it was found that both ORC homologues could inhibit the helicase activity of MCM. Further it was found that ORC2 could autophosphorylate in the presence of ATP and more remarkably could phosphorylate MCM in a species-specific manner.

DNA replication is an essential process in both prokaryotic and eukaryotic organisms that must occur in order for cells to divide and proliferate. The replication process in all organisms begins with the ordered assembly of a multiprotein complex at the replication origin, which in eukaryotes is called the pre-replication complex (pre-RC) (*1*). Several proteins play a crucial role in the formation of the pre-replication complex (pre-RC), including the origin recognition complex (ORC), CDC6, and minichromosome maintenance (MCM) proteins. In yeast, ORC associates with DNA in a sequence-specific manner and recruits the rest of the pre-RC in a cell cycle dependent manner. Archaea, the third kingdom of life, are believed to replicate DNA using proteins with homology to their eukaryotic counterparts (*2*).

Almost all of the archaea for which the genome is known contain a single MCM homologue (*3*), which forms a homohexamer (*4, 5*) or a double homohexamer (*6*). The crystallographic structure of the *Methanothermobacter thermoautotrophicum* (*Mth*) MCM N-terminal portion (residues 2−286) revealed a dodecameric architecture, with two hexameric rings juxtaposed in a head-to-head configuration (*6*). *In vitro* studies have revealed that several archaeal MCM helicases possess biochemical properties similar to those of the eukaryotic MCM helicase (*5, 7*−*14*), including affinity for ssDNA,[1] DNA-stimulated ATPase activity and a 3′−5′ helicase activity, which is dependent upon ATP. Studies on the biochemical properties of euryarchaeal and crenarchaeal MCMs demonstrated similarities and important differences. The biochemical data from euryarchaeal MCMs comes from the characterization of *Methanothermobacter thermoautotrophicum* MCM (*Mth*MCM), *Archaeoglobus fulgidus* MCM (*Af*MCM), and *Thermoplasma acidophilum* MCM (*Tac*MCM) (*15*), while the only crenarchaeal MCM studied to date comes from *Sulfolobus solfataricus (Sso*MCM*)*. Euryarchaeal MCMs bind both single- and double-stranded DNA, independent of metal ions or nucleotide (*10, 15, 23*). Their ATPase activity is stimulated by both single-stranded and double-stranded DNA, while the ATPase activity of the crenarchaeal *Sso*MCM is not but appears highly active without additional DNA (*7*−*9, 11, 13*). Another distinction between the two archaeal kingdoms is the type of the zinc-binding motif: while the euryarchaeal species have a zinc-binding motif of C_4 type, the crenarchaeal ones have an HC_3 type.

In archaea, the interactions among the initiation proteins are currently unclear. Archaeal DNA replication proteins resemble those of eukarya but assume somewhat simpler forms. Within the repertoire of archaeal homologues of eukaryotic replication proteins, the most likely candidates

[†] This work was supported by Cancer Research UK.

* Corresponding author. Present address: Department of Biochemistry, University of Oxford, Oxford OX1 3QU, UK. Phone: (+44) 01865 275734. Fax: (+44) 01865 275297. E-mail: Ian.grainge@bioch.ox.ac.uk.

[‡] Present address: Division of Metabolic Diseases, Department of Laboratory Medicine, Karolinska Institutet, Novum, SE-141 86 Stockholm, Sweden

[1] Abbreviations: ATP, adenosine 5′-triphosphate; bp, base pair; dsDNA, double-stranded DNA; nt, nucleotide; PAGE, polyacrylamide gel electrophoresis; PCR, polymerase chain reaction; ssDNA, single-stranded DNA; WH domain, winged helix domain.

10.1021/bi801479s CCC: $40.75
Published on Web 11/17/2008

for initiator proteins that mediate origin recognition are the archaeal ORC/CDC6 homologues (*16, 17*). Most archaeal species that have been sequenced contain at least one such homologue (*18*). The archaeal ORC/CDC6 proteins are related to both the eukaryotic ORC1 subunit of the origin recognition complex and CDC6. However, for simplicity the archaeal homologues will be referred to as ORC hereafter, with a number defining them if there are more than one present in an organism. Sequence analysis suggests the existence of at least two subfamilies of these proteins. The basis for the division of the subfamilies is a conserved motif that may be a recognition helix (*19*). *In vitro* studies demonstrated that the *M. thermoaoutotrophicum* ORC-1 and ORC-2 proteins inhibit MCM helicase activity, and it was therefore suggested that the proteins interact (*14*). These interactions were confirmed by two-hybrid and Far-Western blot analysis. Conversely, it was seen that one of the ORC homologues from *T. acidophilum* stimulated the MCM helicase activity (*15*), and interaction was demonstrated by two-hybrid and pull-down experiments.

Although the ORC homologues are very similar in primary amino acid sequence (*20*) and were suggested to have similar structure and domain organization (*19*), they appear to employ different regions for MCM binding. While *Mth*ORC-1 binds MCM predominately via the WH domain, this domain of *Mth*ORC-2 alone does not interact with *Mth*MCM (*14*), but interaction is seen when the full length protein is used. This is similar to the observations made with an ORC homologue from *S. solfataricus* in which an indirect assay suggested that the WH domain of one of the three ORC homologues is not required for MCM binding (*21*). The major contact between *Mth*MCM and *Mth*ORC homologues is via the N-terminal portion of MCM (*10, 22*). In contrast, the ORC homologue from *Pyrobaculum aerophilum* was not seen to bind to MCM (*14*).

The crenarchaeote *Aeropyrum pernix* encodes two genes with homology to ORC, called ORC1 and ORC2 (*19*), and a single MCM homologue (*Ape*MCM). We characterize the DNA binding, ATPase, and helicase activites of *Ape*MCM, confirming the activity of the protein. To further characterize the *Ape*MCM, four of the conserved motifs within the protein were mutated: a zinc-binding motif of an HC_3-type, Walker A and Walker B motifs, and a putative arginine finger. The zinc-binding mutant still binds single-stranded and double-stranded DNA but in an ATP-dependent manner and possesses DNA-dependent ATPase activity and limited helicase activity. Mutation of the Walker A, Walker B, and putative arginine finger regions lead to abolition of both ATPase and helicase activity. This suggests that in *Ape*MCM, similar to the eukaryotic MCM2−7 complex, the ATP binding/hydrolysis sites are located at the subunit interface. Data using an N-terminal deletion of 256 amino acids of *Ape*MCM suggest that this region may play a regulatory role; when the N-terminus is deleted, the ATPase activity increases and becomes somewhat uncoupled from DNA binding.

The interactions between *Ape*MCM and the ORC proteins were also studied. Helicase activity of *Ape*MCM was seen to be inhibited by the presence of domain III of the ORC2 protein, and this inhibition is dependent upon the N-terminus of *Ape*MCM. Conversely domains I and II of ORC1 inhibited the helicase activity of *Ape*MCM. Further, the ORC2 protein was capable of autophosphorylation after binding ATP. Intriguingly, ORC2 was also observed to phosphorylate MCM in a species-specific manner: it could phosphorylate *Ape*MCM but not MCM from *A. fulgidus.*

MATERIALS AND METHODS

Radiolabeled and unlabeled ATP were obtained from Amersham Bioscience. Synthetic oligonucleotides were prepared by the Oligosynthesis department (Cancer Research UK) or by Oswel Ltd. and Sigma Genosys Ltd. Sequence alignments were carried out using ClustalW.

Constructing the ApeMCM Mutants. The *Ape*Mcm gene (APE0188) was amplified by PCR from genomic DNA using primers bearing *Nco*I and *Eco*RI sites. The resulting product was cut with *Nco*I and *Eco*RI enzymes, gel purified, and ligated into pET28b vector (Novagen). The ΔN256 MCM gene was cloned using an identical strategy except that a different primer for the N-terminus of the gene was used for the initial PCR reaction. All restriction enzymes used were from New England Biolabs.

All mutations were generated using QuickChange site-directed mutagenesis kit (Stratagene) using pET28b plasmid containing the wild-type gene as a template. Following mutagenesis, the genes were sequenced to ensure that no additional mutations were created.

*Protein Expression and Purification. Ape*MCM and the mutant forms were expressed as described previously (*15*). Cells were lysed with a homogenizer (Stansted Fluid Instruments) at 15 000 psi in the presence of 140 ng/mL pepstatin, 400 ng/mL leupeptin, and 1 mM phenylmethylsulfonyl fluoride (PMSF). Cell debris was removed by centrifugation at 20 000*g*. Supernatant was heat precipitated at 55 °C for 10 min and centrifuged to remove precipitant. Remaining protein was precipitated by the addition of 0.44 g/mL ammonium sulfate. Protein was resuspended in a buffer containing 50 mM Tris, pH 7.5, 1 mM EDTA, and 1 mM DTT, so that the conductivity was 10 mS/cm, and loaded onto a Source30Q column equilibrated with buffer A (50 mM Tris, pH 7.5, 50 mM NaCl, 1 mM EDTA, 1 mM DTT). Protein was eluted with a linear gradient to buffer B (50 mM Tris, pH 7.5, 1 M NaCl, 1 mM EDTA, 1 mM DTT). Fractions containing MCM were pooled, and saturated ammonium sulfate solution was added to bring the final concentration of ammonium sulfate to 1 M. This was then loaded onto a Source Isopropyl column (Pharmacia) in 50 mM Tris, pH 7.5, 1 mM EDTA, 1 mM DTT, and 1 M ammonium sulfate and eluted with a linear gradient to buffer A. Eluate was run on a HiLoad 16/60 Superdex S200 gel-filtration column (Pharmacia) equilibrated in a buffer containing 50 mM Tris, pH 7.5, 500 mM NaCl, 1 mM EDTA, and 1 mM DTT. Protein samples were examined by SDS−PAGE and stained with Coomassie (Figure 1A).

ORC1 and ORC2 proteins were expressed and purified as described previously (*19, 23*).

DNA Substrates. Oligonucleotides were labeled using T4 polynucleotide kinase (New England biolabs) and [γ-^{32}P]ATP (Amersham). Unincorporated nucleotide was removed using a Bio-Rad P6 spin column. For double-stranded substrates, the labeled oligonucleotide was annealed to a 2-fold molar excess of a cold complementary strand by cooling at 1 °C/min from 95 to 25 °C in a PCR machine. DNA sequences used for the DNA binding assays were the same as described previously (*9*).

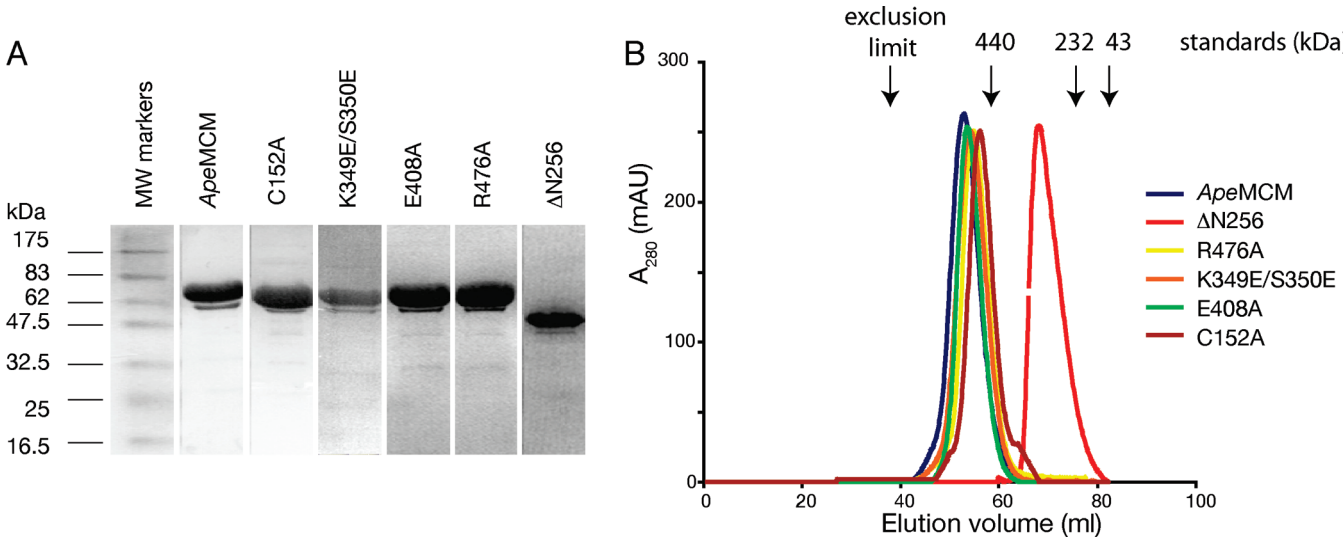

FIGURE 1: Gel filtration analysis of *Ape*MCM protein and its mutants: (A) Coomassie blue-stained SDS−PAGE of the wild-type, zinc, Walker A, Walker B, arginine, and ΔN256 mutant proteins after GF purification procedure. (B) Elution profile of the purified proteins from Superdex S200 (16/60) gel filtration column. The arrows indicate the position of the protein markers used to calibrate the column (blue dextran, ferritin, catalase, and ovalbumin).

DNA Binding Assay. The indicated protein concentrations were incubated with 2.5 nM radioactively labeled DNA in a buffer (25 mM HEPES, pH 7.5, and 25 mM $MgCl_2$) at room temperature for 10 min. The samples were then run on a 6% native polyacrylamide gel to separate the protein−DNA complex from the free DNA. Gels were dried and analyzed with a Storm phosphorimager and ImageQuant software.

DNA binding experiments were repeated in triplicate, and the average and standart deviations from the three data sets were plotted using a best fit line from GraphPad Prism. The data were analyzed using GraphPad Prism and, where appropriate, were fitted to a simple independent binding sites model:

$$\alpha = \alpha_M(([P]_T + [DNA]_T + K_{d(app)}) - (([P]_T + [DNA]_T + K_{d(app)})^2 - 4[P]_T[DNA]_T)^{0.5})/(2[DNA]_T)$$

where α is the percentage of DNA bound, α_M is the percentage of DNA bound at saturation, $[P]_T$ is the total protein concentration, $[DNA]_T$ is the total concentration of DNA, and $K_{d(app)}$ is the apparent dissociation constant.

Sigmoidal curves were fitted to the Hill equation and used to determine the Hill coefficient n, $\alpha = \alpha_M(([P]_T^n)/([P]_T^n) + K)$.

Helicase Assay. Helicase reactions were carried out at 60 °C in a reaction buffer containing 25 mM HEPES, pH 7.5, 25 mM $MgCl_2$, 10 mM ATP, and 10% glycerol using 1 nM DNA substrate and 0.4 μM wt or mutant proteins per hexamer. After a 2 min preincubation at 60 °C, the reactions were started by adding ATP and later stopped by adding stop buffer (to final concentration of 0.1% w/v SDS, 40 mM EDTA, 8% v/v glycerol, 0.01% w/v bromophenol blue). Where indicated, 2.8 μM *A. pernix* ORC1 and ORC2 proteins or their deletion mutants were added. Displaced oligonucleotide was separated from substrate by electrophoresis through a 10% nondenaturing polyacrylamide gel at 150 V. Gels were then dried and exposed to a phosphorimager cassette. Quantitive analysis was performed with a phosphorimager and ImageQuant software. Strand displacement is measured as a percentage by determining the counts associated with displaced oligonucleotide and the total counts associated with both annealed and displaced oligonucleotide in each lane.

ATPase Reactions. ATP hydrolysis was determined by using an ammonium molybdate−malachite green based method for assaying nanomolar quantities of inorganic phosphate as described previously (*24*). Malachite green solution (0.045%) was mixed immediately prior to use with 5% $(NH_4)_6Mo_7O_{24}$ in 4 M H_2SO_4 in a 3:1 ratio. The resulting solution was filtered through a 0.2 μm syringe filter. Initially, various concentrations of the wt protein were used to assess the appropriate amount of protein at a given time point to be within the linear response region of the assay. Subsequent reactions were carried out in this range. Reactions were at 75 °C in 50 μL volume for 10 min. Each reaction contained 20 pmol/hexamer in the buffer described for DNA binding and was incubated at reaction temperature for 5 min prior to addition of ATP. At the appropriate time after addition of ATP, reactions were mixed with 800 μL of malachite green solution for 1 min at room temperature. Sodium citrate (100 μL, 34% w/v) was added, and color development was allowed to proceed for 20 min. Optical densities at 660 nm were taken and normalized to a control reaction of ATP in buffer without protein. For reactions with DNA, either 40 pmol of oligonucleotide or an excess of sonicated salmon sperm DNA was added to the reaction mixture.

Phosphorylation Reaction. Phosphorylation assays for *A. pernix* ORC2 protein were performed at 75 °C for 10 min and for ORC1 protein for 5 h. The proteins were incubated in a reaction mixture (10 μL volume) containing 1.4 μM [γ-^{32}P]ATP in 25 mM HEPES, pH 7.5, and 25 mM $MgCl_2$, in the presence or absence of 5.6 μM single-stranded or double-stranded DNA (ORB1). Unless otherwise stated, *A. pernix* MCM protein was used at a concentration of 0.46 μM hexamer; *A. pernix* ORC2 and ORC1 proteins and their deletions mutants were used at concentrations of 2.8 μM per reaction. The proteins were then separated by 12% SDS−PAGE gel, and the ^{32}P-labeled bands were detected using a phosphorimager.

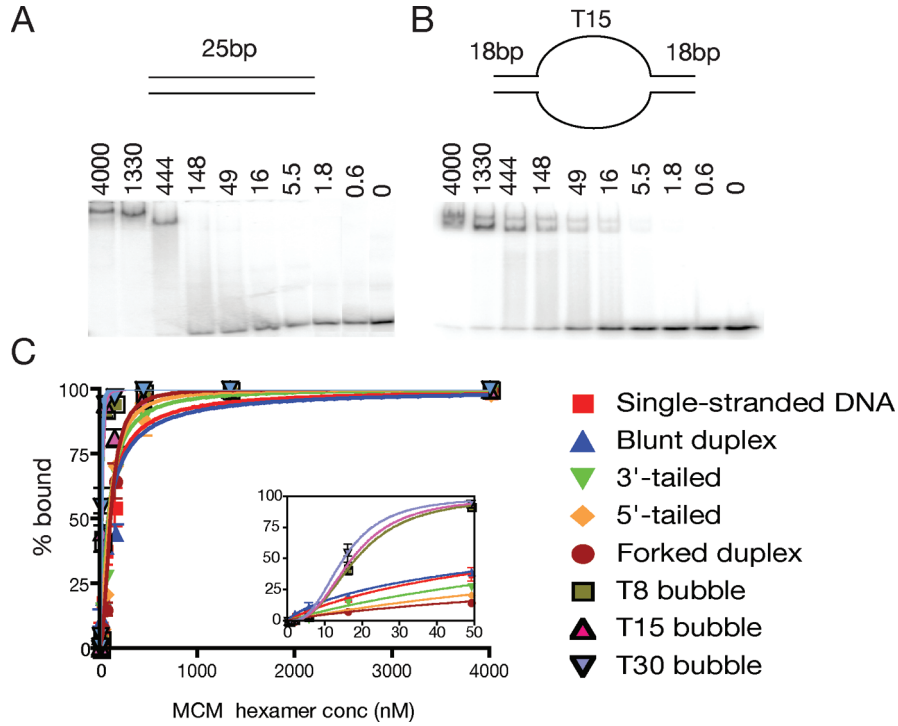

FIGURE 2: Binding of *Ape*MCM to various DNA substrates: DNA binding gel of *Ape*MCM (A) to a linear duplex and (B) to a bubble containing 15 T's on each strand flanked by 18 bp of DNA duplex; (C) graphs showing variation in DNA binding at concentrations up to 4000 nM hexamer. The inset of the graph shows an enlarged view of DNA binding at lower concentrations. The percentage bound represents substrate shifted to both complexes. The plots show the average and standard deviations from three independent experiments. Cooperative binding between two hexamers was observed only on bubble substrates.

To detect possible amino acid residues of *Ape*MCM protein phosphorylated by *A. pernix* ORC2, an MCM peptide membrane array was used (Protein and Peptide Chemistry Laboratory, CR UK). The phosphorylation reaction was done as described above in total volume of 3 mL. The membrane containing the *Ape*MCM peptides was covered with the reaction mixture and incubated for 30 min in a 75 °C water bath. The membrane was washed five times with 10 mM EDTA, followed by washing with 3% SDS and then with 1.5 M NaCl. To remove any nonspecifically bound ATP, the membrane was washed overnight at room temperature with 500 mM phosphoric acid. The membrane was then washed first with water, then with ethanol, dried, and exposed overnight to a phosphorimager cassette.

Processivity Assay. Substrates and reaction conditions were as described previously (*9*).

RESULTS AND DISCUSSION

Cloning of ApeMCM and Site-Specific Mutations. Analysis of the *A. pernix* genome sequence revealed the presence of a single open reading frame coding for a putative homologue of the eukaryotic MCM proteins (APE0188). Sequence alignment of archaeal MCMs and MCM4 from *Homo sapiens* and *Saccharomyces cerevisiae* showed that *Ape*MCM shares 32% identity with the human and yeast MCM4. *Ape*MCM does not contain the N-terminal extension of about 160 amino acid residues found in the eukaryotic counterparts, which contains the majority of the cyclin-dependent kinase phosphorylation sites (*25, 26*). Moreover, the core region of the archaeal and eukaryal sequences show a higher level of similarity because they contain the conserved amino acid motifs typically found in DNA helicases (*27*). These include the Walker A and B motifs that are responsible for nucleotide binding and hydrolysis, respectively (*28*), and an arginine finger motif toward the C-terminus of the protein. In addition, the *Ape*MCM sequence contains a zinc-binding motif of the HC_3-type, whereas the MCM proteins from eukaryotic organisms (*26, 28*) and the euryarchaeal species (*12*) possess a zinc-binding motif of the C_4-type.

Each of these four conserved motifs was mutated separately in *Ape*MCM. The wild-type *Ape*MCM, C152A (zinc-binding mutant), K349E/S350E (Walker A mutant), E408A (Walker B mutant), R476A (arginine mutant), and ΔN256MCM (deletion mutant) were overexpressed and purified from *Escherichia coli* (Figure 1A).

ApeMCM and the Mutant Derivatives Form Hexamers in Solution. In order to assess the oligomeric state of the recombinant *Ape*MCM and the point mutants, each was analyzed by gel filtration on a Superdex S200 (16/60) column (Figure 1B). A set of globular protein standards was run under the same experimental conditions, and the apparent molecular weights of the MCM proteins are calculated from the equation of this standard calibration curve. A molecular mass of about 480 kDa was estimated, which suggests that *Ape*MCM and its mutants form hexamers in solution. The ΔN256MCM deletion mutant also formed hexamers (calculated apparent molecular weight of 294 kDa).

DNA Binding Properties of ApeMCM. The ability of the wild-type *Ape*MCM protein to bind single-stranded and double-stranded DNA was investigated by incubating ^{32}P-labeled oligonucleotides with increasing amounts of protein (concentrations 0−4000 nM) (Figure 2) in the presence and absence of ATP. A variety of DNA substrates were used to assay the binding preference of the wild-type *Ape*MCM (*9*).

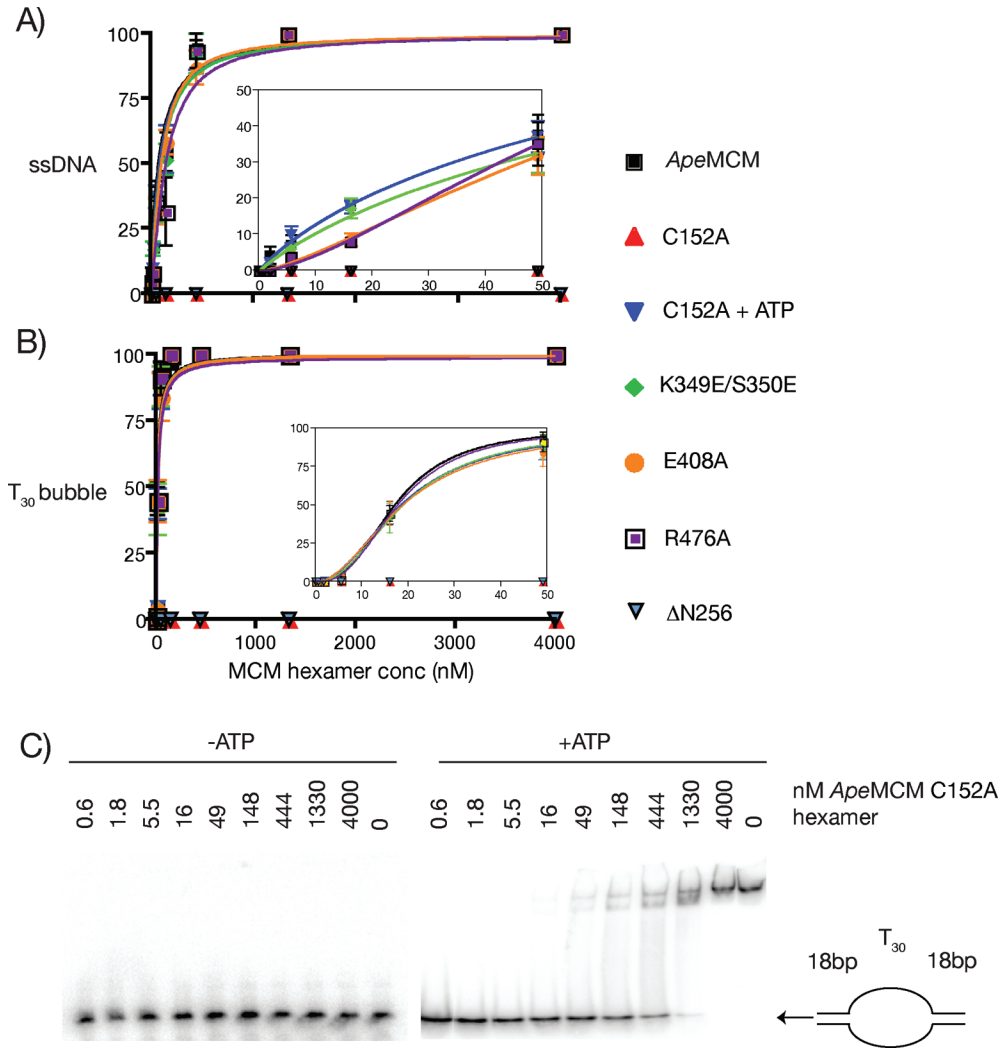

FIGURE 3: Graphic representation of the DNA binding activity of *Ape*MCM and its mutant proteins: (A) binding to a single-stranded 25 base long DNA; (B) binding to T30 bubble. The insets of the graphs represent an enlarged view of DNA binding at concentrations up to 50 nM per hexamer. The percentage bound represents substrate shifted by the two complexes. Cooperative binding between two hexamers was observed only on the bubble substrate (C).

These encompassed substrates of single-stranded or double-stranded DNA or substrates containing both (forked duplex with 25 bp duplex and 20 nt single-stranded arms). To quantitatively analyze the data for these interactions, the binding curves were fitted to an independent binding site equation and the Hill equation when possible. All of the different substrates in the assays were bound by the wild-type enzyme (Figure 2) in a concentration-dependent manner. Furthermore, this binding was not affected by the presence of ATP (data not shown). In substrates containing only 25 bases of single-stranded or double-stranded DNA, a single-band was observed on the polyacrylamide gels (Figure 2A). The migration of this band however decreases at the highest protein concentrations, which may indicate that more than one hexamer is associated in these complexes in some way. However, on larger substrates two complexes are seen, which is interpreted as two hexamers binding to a single substrate (Figure 2B). In the plot, the amount bound represents substrate shifted to both complexes (Figure 2C). Although binding to a variety of double-stranded DNA structures was analyzed, there was very little variation in binding efficiency between them, with the exception of those containing a single-stranded bubble flanked by duplex DNA. This suggests that a bubble substrate is a preferred ligand for the MCM hexamer. Cooperative binding between hexamers was observed on bubble substrates that is absent on the other DNA substrates. Furthermore, the size of the single-stranded region of the bubble affects the affinity: an increase of the single-stranded bubble region led to increased affinity. Hill coefficients were 2.9 ± 0.2 for an 8 base bubble, 3.3 ± 0.1 for a 15 base bubble, and 4.3 ± 0.2 for a 30 base bubble.

The Walker A, Walker B, and arginine finger mutants bind DNA with the same affinity as wt *Ape*MCM, forming two distinct bands on DNA substrates longer than 25 bases (Figure 3A,B). Only the zinc-binding mutant was unable to bind single-stranded or double-stranded DNA in the absence of ATP. The addition of ATP however stimulated its binding to both substrates (Figure 3C). A similar observation was reported for the zinc-binding mutant of *M. thermoautotrophicum* MCM, where the presence of ATP increased the single-stranded DNA binding affinity of the mutant protein (*12*), although in this case, some binding was observed in the absence of ATP.

The N-terminal deletion mutant of *Ape*MCM did not bind single-stranded or double-stranded DNA. Presumably the N-terminus contributes considerably to the DNA binding potential of the MCM hexamer either directly through

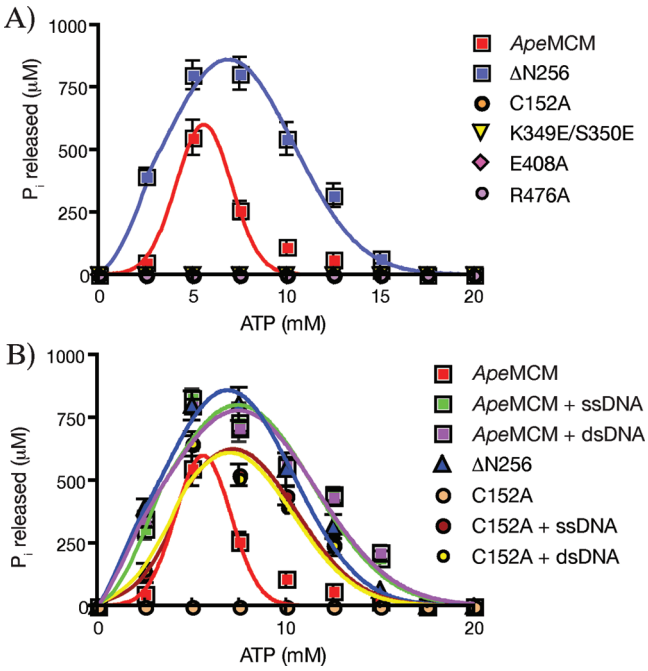

FIGURE 4: ATPase activity of *Ape*MCM: (A) comparison of the ATPase activity of the wild-type *Ape*MCM and its mutants; (B) the effect of single-stranded and double-stranded DNA on the ATPase activity of the wild-type *Ape*MCM and the zinc mutant in comparison to the ATPase activity of ΔN256 mutant.

contacting DNA or indirectly by stabilizing the hexamer on DNA rather like a processivity factor.

ATPase Activity of ApeMCM. The ATPase activity of each mutant protein was compared with that of the wild-type *Ape*MCM in the presence or absence of DNA. The wild-type enzyme showed a reasonable level of activity in the absence of DNA (Figure 4A), but was stimulated by both ssDNA and dsDNA to a similar degree (Figure 4B). This is in agreement with the observations made on a euryarchaeal MCM (*9*), but in contrast to the observations on another creanarchaeal protein, which suggested that the ATPase activity of *S. solfataricus* MCM is not affected by the presence of ss- or dsDNA (*7*). The ΔN256 mutant gave robust activity both in the presence and absence of DNA and gave an ATPase profile similar to that of the wild-type MCM when stimulated by DNA (Figure 4A,B). The wild-type *Ape*MCM exhibits two levels of ATPase activity, one that is independent of DNA being bound, and a higher activity that is seen upon DNA binding. Seemingly the deletion of the N-terminus of the protein has removed the DNA dependence from ATPase activity, and the ATPase rate for this deletion mutant is up to the DNA-stimulated rate of the wild-type enzyme. One explanation is that the N-terminus acts as a negative regulator of the ATPase activity in the absence of DNA and that DNA binding relieves any negative inhibition.

As expected, the K349E/S350E, E408A, and R476A mutants failed to give any detectable ATPase activity, confirming the vital role of these active site residues. In the absence of DNA, the C152A mutant also failed to hydrolyze ATP. However, in the presence of either ssDNA or dsDNA, it did hydrolyze ATP, with both DNAs stimulating activity to a similar level. ATP hydrolysis by this mutant in the presence of DNA was marginally lower than that observed with wild-type *Ape*MCM but showed a similar dependence upon ATP concentration. The stringency of dependence of this mutant's ATPase activity upon DNA may reflect a greater dependence for stable hexamerization upon DNA binding. Alternatively, DNA binding may lead to an activating conformational change that is partially bypassed in the wild-type enzyme. Further, the binding to DNA of this mutant was itself dependent upon ATP (Figure 3C), suggesting an interdependence between ATP binding, DNA binding, and ATP hydrolysis.

Helicase Activity of the ApeMCM Mutants. The recombinant wild-type and mutant *Ape*MCM proteins were tested for DNA helicase activity by a strand-displacement assay performed at 60 °C for 30 min. Forked and blunt duplex DNA substrates were used in these assays. *Ape*MCM showed robust helicase activity on the forked DNA duplex (Figure 5A) but was unable to unwind the blunt DNA duplex (data not shown). The variation of wild-type MCM helicase activity on the forked substrate with different concentrations of ATP was also analyzed (Figure 5A,B). The optimal range for efficient helicase activity appears to be between 5 and 12.5 mM ATP, and activity drops off dramatically outside this range. This is in reasonable agreement with the range of ATP concentrations that gave good ATPase activity (Figure 4B).

The helicase activities of the wild-type and mutant proteins were also compared (Figure 5C,D). As expected the catalytic mutants, which demonstrated no ATPase activity, resulted in proteins unable to unwind DNA. ΔN256 MCM had a higher activity than the wild-type protein under these conditions, correlated with its higher ATPase activity, despite having shown no demonstrable DNA binding activity. Presumably the loss of the N-terminal portion of the protein reduces the stability of the protein−DNA complex such that it cannot be detected by a gel-based assay but it is sufficiently stable to allow unwinding of these short substrates.

*Ape*MCM was also tested for its ability to unwind longer regions of DNA, using an assay previously described (*9*). It was found to be able to displace duplex DNA up to 1 kb in length (the longest tested), showing that it has reasonable processivity (data not shown).

ApeORC1 and ApeORC2 Proteins Inhibit the Helicase Activity of ApeMCM. The helicase assay with *Ape*MCM was repeated in the presence of ORC1 and ORC2 proteins and deletion derivatives thereof. As Figure 6A shows, both full length ORC2 and domain III of ORC2 inhibit the helicase activity of the wild-type MCM but not that of ΔN256 MCM. Consistent with this are previous observations suggesting that the main contact between MCM and ORC2 is via the N-terminal portion of MCM protein and the winged helix domain of ORC2 (*10*). ORC1 protein also inhibited the helicase activity of the *Ape*MCM but not of the ΔN256 MCM. However, even domains I and II of ORC1 inhibited the helicase activity of MCM (Figure 6B) suggesting that within domains I and II, there is another MCM interaction site.

Phosphorylation of ApeMCM by ORC2. The two ORC homologues from *M. thermoautotrophicum* are able to undergo an autophosphorylation reaction *in vitro* that requires a γ-phosphate of ATP or dATP and an intact Walker A motif (*10, 29*). A phosphoamino acid analysis with acid hydrolysis and one-dimensional electrophoresis revealed that both proteins are phosphorylated on serine residues, but the

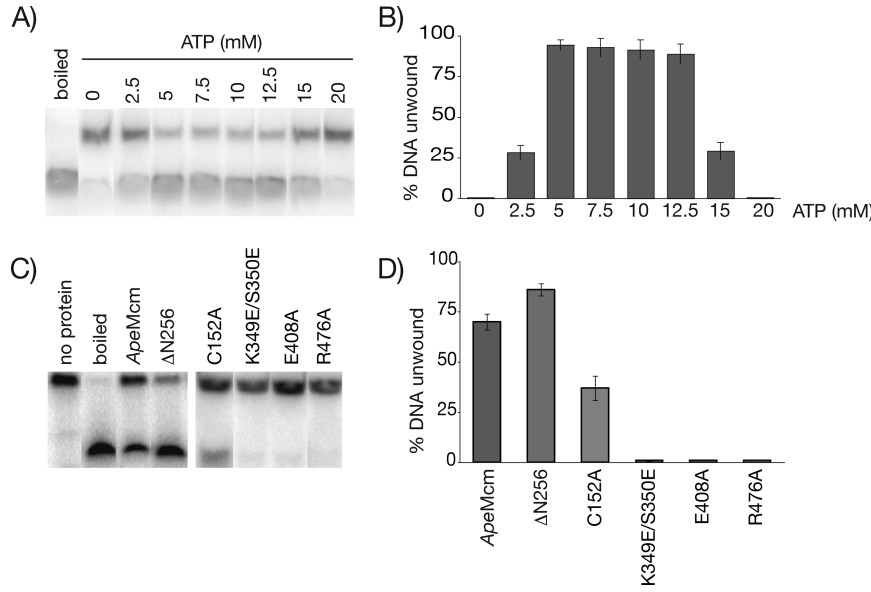

FIGURE 5: Helicase assay for *Ape*MCM: (A) the effect of ATP concentration on the helicase activity of *Ape*MCM assayed on a flayed duplex duplex DNA substrate; (B) graphic representation of the effect of ATP concentration on helicase activity of the wild-type enzyme; each bar is the average of three independent experiments; (C) representative autoradiograph of the helicase activity of the wild-type and mutant proteins in the presence of 5 mM ATP on a flayed duplex DNA; (D) graphic representation of three repetitions of the assay shown in panel C.

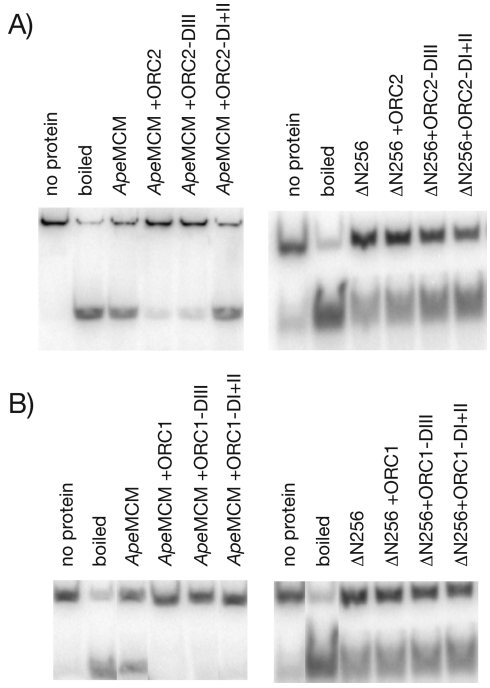

FIGURE 6: Helicase assay for *Ape*MCM and ΔN256 mutant on a flayed duplex DNA in the presence of 5 mM ATP (A) in the presence of ORC2 or (B) in the presence of ORC1.

precise location of the phosphorylation sites is unknown (*29*). It was found that ss- and dsDNA inhibits the autophosphorylation of both ORC homologues from *M. thermoautotrophicum*. Autophosphorylation of ORC was also reported for one of the crenarchaeal *S. solfataricus* ORC homologues (*21*) and for the ORC homologue of *P. aerophilum* (*29*). Autophosphorylation of *Sso*ORC required a functional Walker A motif, but ss- and dsDNA inhibited this activity only slightly (*21*). Autophosphorylation activity was observed for the eukaryal CDC6 protein as well (*29*), with phosphorylation of both serine and threonine residues.

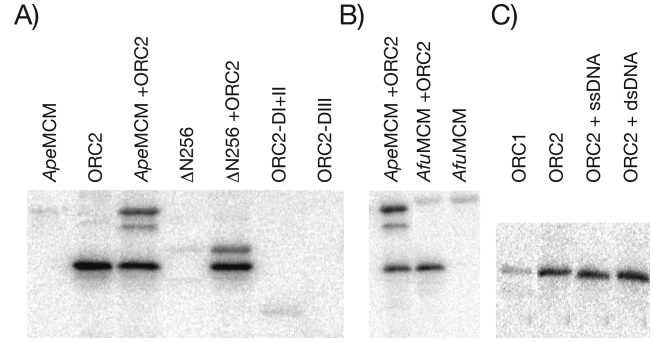

FIGURE 7: Phosphorylation assays (A) within *A. pernix* proteins and (B) with MCM from *A. fulgidus*. Only the full length ORC2 phosphorylates itself and *Ape*MCM but not *Af*MCM. (C) ORC1 did not undergo phosphorylation, and ss- or dsDNA did not have any effect on the phosphorylation of ORC2.

To examine whether the *A. pernix* ORC homologues undergo autophosphorylation, the proteins were incubated in the presence of [γ-^{32}P]ATP at 75 °C. As Figure 7 shows, a low level of autophosphorylation was observed only for *Ape*ORC2,but not for the *Ape*ORC1 protein. Only the full-length ORC2 was able to undergo phosphorylation; the mutant with domains I and II alone was not able to autophosphorylate, suggesting that the ORC2 phosphorylation sites may be located within domain III or that all three domains are required for catalytic activity. In contrast to the observation for *M. thermoautotrophicum* and *S. solfataricus* ORC homologues, ss- and dsDNA did not inhibit the autophosphorylation ability of *Ape*ORC2 (Figure 7C). In eukaryotes, ORC and CDC6 are phosphorylated by cyclin-dependent kinases (*30, 31*). Phosphorylation of CDC6 is associated with its degradation (in yeast) or nuclear export (in mammals) (*32*−*34*). Since CDC6 is essential for MCM to load onto chromatin, this has the effect of restricting MCM loading to G1/S, when CDC6 is present and active. Therefore, it was proposed that autophosphorylation in archaea might play a regulatory role during initiation as well (*3, 29, 35*).

It was also hypothesized that ORC−MCM interaction may regulate the phosphorylation activity during assembly of the helicase around DNA at the origin (*35*). Thus, the effect of MCM on the ORC autophosphorylation was analyzed. In contrast to the observations for the *M. thermoautotrophocum* ORC homologues, where MCM stimulated the autophosphorylation of ORC1 but inhibited the autophosphorylation of ORC2 (*10*), MCM from *A. pernix* did not affect the level of autophosphorylation of *Ape*ORC2 (Figure 7A). However, it was found that ORC2 phosphorylates full-length MCM and MCM in which the N-terminal 256 amino acids were deleted (Figure 7A). Further, there is species specificity in this MCM phosphorylation since the *A. fulgidus* MCM was not phosphorylated by the *Ape*ORC2 (Figure 7B).

The low level of phosphorylation made it very difficult to locate the phosphorylation sites of either MCM or ORC2 in the intact protein. To detect possible phosphorylation sites within *Ape*MCM, 16 amino acid long peptides (which overlap every two amino acids) from *Ape*MCM were spotted on a filter membrane. This membrane was used in the radioactive phosphorylation reaction as above. Several regions of the membrane showed phosphorylation by ORC2, indicating several potential sites, involving serine, threonine, and tyrosine residues (Figure S1, Supporting Information). As yet, the significance of these phosphorylated residues is unknown.

It is tantalizing to speculate that these phosphorylation reactions may have a role *in vivo* in the control of both origin licensing activity of the ORC proteins and the helicase activity of the MCM protein. However, at present both activites *in vitro* appear to be rather inefficient. Ideally, these potential activites would be investigated further, within the living organism, but as yet the genetic tools are unavailable to do so in *A. pernix*. However, these techniques are becoming available within related archaea. Several other proteins, such as the homologues of the GINS complex (*36*), are believed to be involved during the assembly of an active replication origin in archaea. It is possible that within the context of a properly ordered complex on origin DNA these reactions may become significant. If so, then do similar levels of control occur with eukaryotic organisms? Subunits of the MCM2−7 complex are phosphorylated by cyclin-dependent kinases to regulate both chromatin binding and helicase activity (*32, 37*−*39*), but as yet there have been no indications that ORC/CDC6 proteins contribute directly to MCM2−7 phosphorylation.

ACKNOWLEDGMENT

We thank D. Wigley for help, support, and discussion during this project and J. Diffley for his kind support.

SUPPORTING INFORMATION AVAILABLE

Dot blot assay of phosphorylation of an *Ape*MCM peptide array by ORC-2 protein. This material is available free of charge via the Internet at http://pubs.acs.org.

REFERENCES

1. Bell, S. P., and Dutta, A. (2002) DNA replication in eukaryotic cells. *Annu. Rev. Biochem. 71*, 333–374.
2. Barry, E. R., and Bell, S. D. (2006) DNA replication in the archaea. *Microbiol. Mol. Biol. Rev. 70*, 876–887.
3. Kelman, L. M., and Kelman, Z. (2003) Archaea: An archetype for replication initiation studies? *Mol. Microbiol. 48*, 605–615.
4. Chen, Y. J., Yu, X., Kasiviswanathan, R., Shin, J. H., Kelman, Z., and Egelman, E. H. (2005) Structural polymorphism of *Methanothermobacter thermautotrophicus* MCM. *J. Mol. Biol. 346*, 389–394.
5. McGeoch, A. T., Trakselis, M. A., Laskey, R. A., and Bell, S. D. (2005) Organization of the archaeal MCM complex on DNA and implications for the helicase mechanism. *Nat. Struct. Mol. Biol. 12*, 756–762.
6. Fletcher, R. J., Bishop, B. E., Leon, R. P., Sclafani, R. A., Ogata, C. M., and Chen, X. S. (2003) The structure and function of MCM from archaeal *M. thermoautotrophicum*. *Nat. Struct. Biol. 10*, 160–167.
7. Carpentieri, F., De Felice, M., De Falco, M., Rossi, M., and Pisani, F. M. (2002) Physical and functional interaction between the minichromosome maintenance-like DNA helicase and the single-stranded DNA binding protein from the crenarchaeon *Sulfolobus solfataricus*. *J. Biol. Chem. 277*, 12118–12127.
8. Chong, J. P., Hayashi, M. K., Simon, M. N., Xu, R. M., and Stillman, B. (2000) A double-hexamer archaeal minichromosome maintenance protein is an ATP-dependent DNA helicase. *Proc. Natl. Acad. Sci. U.S.A. 97*, 1530–1535.
9. Grainge, I., Scaife, S., and Wigley, D. B. (2003) Biochemical analysis of components of the pre-replication complex of *Archaeoglobus fulgidus*. *Nucleic Acids Res. 31*, 4888–4898.
10. Kasiviswanathan, R., Shin, J. H., and Kelman, Z. (2005) Interactions between the archaeal Cdc6 and MCM proteins modulate their biochemical properties. *Nucleic Acids Res. 33*, 4940–4950.
11. Kelman, Z., Lee, J. K., and Hurwitz, J. (1999) The single minichromosome maintenance protein of *Methanobacterium thermoautotrophicum* DeltaH contains DNA helicase activity. *Proc. Natl. Acad. Sci. U.S.A. 96*, 14783–14788.
12. Poplawski, A., Grabowski, B., Long, S. E., and Kelman, Z. (2001) The zinc finger domain of the archaeal minichromosome maintenance protein is required for helicase activity. *J. Biol. Chem. 276*, 49371–49377.
13. Shechter, D. F., Ying, C. Y., and Gautier, J. (2000) The intrinsic DNA helicase activity of *Methanobacterium thermoautotrophicum* delta H minichromosome maintenance protein. *J. Biol. Chem. 275*, 15049–15059.
14. Shin, J. H., Grabowski, B., Kasiviswanathan, R., Bell, S. D., and Kelman, Z. (2003) Regulation of minichromosome maintenance helicase activity by Cdc6. *J. Biol. Chem. 278*, 38059–38067.
15. Haugland, G. T., Shin, J. H., Birkeland, N. K., and Kelman, Z. (2006) Stimulation of MCM helicase activity by a Cdc6 protein in the archaeon *Thermoplasma acidophilum*. *Nucleic Acids Res. 34*, 6337–6344.
16. Edgell, D. R., and Doolittle, W. F. (1997) Archaea and the origin(s) of DNA replication proteins. *Cell 89*, 995–998.
17. Leipe, D. D., Aravind, L., and Koonin, E. V. (1999) Did DNA replication evolve twice independently? *Nucleic Acids Res. 27*, 3389–3401.
18. Myllykallio, H., and Forterre, P. (2000) Mapping of a chromosome replication origin in an archaeon: Response. *Trends Microbiol. 8*, 537–539.
19. Singleton, M. R., Morales, R., Grainge, I., Cook, N., Isupov, M. N., and Wigley, D. B. (2004) Conformational changes induced by nucleotide binding in Cdc6/ORC from *Aeropyrum pernix*. *J. Mol. Biol. 343*, 547–557.
20. Giraldo, R. (2003) Common domains in the initiators of DNA replication in Bacteria, Archaea and Eukarya: Combined structural, functional and phylogenetic perspectives. *FEMS Microbiol. Rev. 26*, 533–554.
21. De Felice, M., Esposito, L., Pucci, B., Carpentieri, F., De Falco, M., Rossi, M., and Pisani, F. M. (2003) Biochemical characterization of a CDC6-like protein from the crenarchaeon *Sulfolobus solfataricus*. *J. Biol. Chem. 278*, 46424–46431.
22. Kasiviswanathan, R., Shin, J. H., Melamud, E., and Kelman, Z. (2004) Biochemical characterization of the *Methanothermobacter thermautotrophicus* minichromosome maintenance (MCM) helicase N-terminal domains. *J. Biol. Chem. 279*, 28358–28366.
23. Grainge, I., Gaudier, M., Schuwirth, B. S., Westcott, S. L., Sandall, J., Atanassova, N., and Wigley, D. B. (2006) Biochemical analysis of a DNA replication origin in the archaeon *Aeropyrum pernix*. *J. Mol. Biol. 363*, 355–369.
24. Lanzetta, P. A., Alvarez, L. J., Reinach, P. S., and Candia, O. A. (1979) An improved assay for nanomole amounts of inorganic phosphate. *Anal. Biochem. 100*, 95–97.

25. Kearsey, S. E., and Labib, K. (1998) MCM proteins: Evolution, properties, and role in DNA replication. *Biochim. Biophys. Acta 1398*, 113–136.
26. Tye, B. K. (1999) MCM proteins in DNA replication. *Annu. Rev. Biochem. 68*, 649–686.
27. Koonin, E. V. (1993) A common set of conserved motifs in a vast variety of putative nucleic acid-dependent ATPases including MCM proteins involved in the initiation of eukaryotic DNA replication. *Nucleic Acids Res. 21*, 2541–2547.
28. Neuwald, A. F., Aravind, L., Spouge, J. L., and Koonin, E. V. (1999) AAA+: A class of chaperone-like ATPases associated with the assembly, operation, and disassembly of protein complexes. *Genome Res. 9*, 27–43.
29. Grabowski, B., and Kelman, Z. (2001) Autophosphorylation of archaeal Cdc6 homologues is regulated by DNA. *J. Bacteriol. 183*, 5459–5464.
30. Elsasser, S., Lou, F., Wang, B., Campbell, J. L., and Jong, A. (1996) Interaction between yeast Cdc6 protein and B-type cyclin/Cdc28 kinases. *Mol. Biol. Cell 7*, 1723–1735.
31. Findeisen, M., El-Denary, M., Kapitza, T., Graf, R., and Strausfeld, U. (1999) Cyclin A-dependent kinase activity affects chromatin binding of ORC, Cdc6, and MCM in egg extracts of *Xenopus laevis*. *Eur. J. Biochem. 264*, 415–426.
32. Fujita, M. (1999) Cell cycle regulation of DNA replication initiation proteins in mammalian cells. *Front. Biosci. 4*, 816–823.
33. Lopez-Girona, A., Mondesert, O., Leatherwood, J., and Russell, P. (1998) Negative regulation of Cdc18 DNA replication protein by Cdc2. *Mol. Biol. Cell 9*, 63–73.
34. Muzi Falconi, M., Brown, G. W., and Kelly, T. J. (1996) cdc18+ regulates initiation of DNA replication in *Schizosaccharomyces pombe*. *Proc. Natl. Acad. Sci. U.S.A. 93*, 1566–1570.
35. Grabowski, B., and Kelman, Z. (2003) Archeal DNA replication: Eukaryal proteins in a bacterial context. *Annu. Rev. Microbiol. 57*, 487–516.
36. Marinsek, N., Barry, E. R., Makarova, K. S., Dionne, I., Koonin, E. V., and Bell, S. D. (2006) GINS, a central nexus in the archaeal DNA replication fork. *EMBO Rep. 7*, 539–545.
37. Coue, M., Kearsey, S. E., and Mechali, M. (1996) Chromotin binding, nuclear localization and phosphorylation of *Xenopus* cdc21 are cell-cycle dependent and associated with the control of initiation of DNA replication. *EMBO J. 15*, 1085–1097.
38. Musahl, C., Schulte, D., Burkhart, R., and Knippers, R. (1995) A human homologue of the yeast replication protein Cdc21. Interactions with other Mcm proteins. *Eur. J. Biochem. 230*, 1096–1101.
39. Young, M. R., and Tye, B. K. (1997) Mcm2 and Mcm3 are constitutive nuclear proteins that exhibit distinct isoforms and bind chromatin during specific cell cycle stages of *Saccharomyces cerevisiae*. *Mol. Biol. Cell 8*, 1587–1601.

BI801479S